On the Stability of Hydride Configurations on Silicon Cluster Surfaces: A First-Principle Theoretical Study

R. Q. Zhang,* W. C. Lu, Y. L. Zhao, and S. T. Lee

Centre Of Super-Diamond and Advanced Films (COSDAF) and Department of Physics and Materials Science, City University of Hong Kong, Hong Kong SAR, China

Received: August 12, 2003; In Final Form: December 7, 2003

The Si−H bond energies and wet oxidation of SiH_x ($x = 1-3$) configurations on silicon cluster surfaces have been studied by ab initio calculations. It is found that the Si−H bond energy is simply determined by its local configuration and is about 75.2 to ∼76.3 kcal/mol for silicon monohydride, 77.9 to ∼78.9 kcal/mol for silicon dihydride, and 80.9 to ∼81.6 kcal/mol for silicon trihydride. The evaporation energies of a hydrogen molecule from the dihydride and trihydride configurations are found to be slightly higher than the calculated bond energies. However, when a water molecule reacts with them, the reaction energy barriers are found to be generally smaller than 50.0 kcal/mol, much less than these bond energies. The calculated reaction barriers and heats do not show clear relationships with the bond energies. Rather, the results show that the reaction at SiH_2 is the most unfavorable one whereas the most easy reaction may take place at the Si−Si dimer on a (2×1) reconstructed Si(001)-like configuration. Our results indicate that the degradation of hydrogenated silicon nanostructures or bulk silicon surfaces might be significantly determined by the possibility of reaction with water molecules, a hydrogenated surface covered by dihydride configurations being the most inert case.

1. Introduction

Hydrogenation is a simple method to stabilize silicon surfaces against oxidation.[1] It can be achieved simply after etching of the silicon surfaces in an aqueous HF acid followed by rinsing in H_2O.[2] Hydrogen-terminated silicon surfaces are constantly attracting intensive study because of their great technological importance in microelectronics. They are also crucial in determining the growth mode of heteroepitaxy.[3] Today, the hydrogenation of silicon surfaces is a controllable process with respect to the surface smoothness and the type of hydrides.[4] Ideal hydrogen termination of the Si (111) surface by monohydride existing on the entire surface can be achieved with low defect and impurity density as well as good stability.[5] However, oxidation processes still take place on a hydrogen-terminated[6] atomically flat silicon surface,[7] whether produced by HF treatment or by surface passivation.[8]

Hydrogen terminations are also the natural product in light-emitting porous silicon,[9] which can be prepared simply by electrochemical etching and has stimulated intensive studies because of its potential applications in silicon-based optoelectronic devices.[10−12] The passivation provided by hydrogen from the electrolyte is very efficient in a fresh sample but unstable.[13] In the same family of nanostructured materials, one-dimensional silicon nanowire is considered promising for its inherent quantum confinement effect in the other two dimensions.[14] Large-scale synthesis, which is always an essential requirement for wide applications, of silicon nanowires has recently been achieved routinely.[15] However, problems of degradation[16] and low photoluminescence (PL) efficiency[17] from the silicon nanostructures remain unsolved. One possible solution is to passivate the silicon surface with elements other than hydrogen. Among the existing passivation methods, nitridation is generally believed to be of advantage.[18] However, there is a technological complication with the removal of the surface oxide layer in order to achieve a satisfactory nitriding effect. We recently reported the carbidation treatment of silicon nanowires and have achieved significantly enhanced and stable PL.[19] An optimal carbidation and a reduced damage during the surface treatment still require intensive study. Nevertheless, the problem of stability has not yet been satisfactorily solved, and further effort is still needed to make the promising silicon nanostructures applicable for the widely desired nanotechnology, in addition to the advancement of conventional microelectronics. The most desirable solution would be that an ideally terminated, nonreactive silicon surface could be still achieved by hydrogen, which has been the driving force for much of the effort expended in surface science in the past 40 years[20] and still deserves pursuing. Recent studies indicate that the stability of hydrogenated silicon nanostructures may be considerably increased compared to that of a hydrogenated silicon wafer.[21,22] In order to reach the goal, a deeper understanding of the hydrogenated silicon surfaces with respect to their bonding and chemical reaction with ambient gases would be crucially important.

Numerous experimental and theoretical research papers have been published about hydrogen adsorptions on clean and reconstructed Si surfaces and the related hydrogen binding energies.[4,23] However, there is no systematic study on the relative bond strength among the SiH_x ($x = 1-3$) configurations, although the study is important for figuring out a stable hydrogenated surface. On the other hand, although the silicon surface oxidation, in which water reaction may take the key role, has been intensively studied also both experimentally and theoretically,[24,25] most of the research work was directed to the water adsorption and dissociation on clean silicon surfaces.[26] Our recent theoretical work has revealed the size dependence of the reactivity of a water molecule interacting with small

* Author to whom correspondence should be addressed. E-mail: aprqz@cityu.edu.hk.

10.1021/jp0364001 CCC: $27.50
Published on Web 01/15/2004

silicon clusters.[22] A systematic investigation about the water reaction on hydrogenated silicon cluster surfaces is still lacking.

In this work, we compare the bond energies of the various hydride configurations which possibly exist on various silicon cluster or nanowire surfaces. In conjunction with a further study on the reaction of a water molecule on them as well as on the related Si−Si backbone, the stability of hydride configurations and the origin of surface degradation are explored.

2. Computational Method

Ab initio molecular orbital calculations were carried out using the GAUSSIAN 98 package.[27] The structures of all the model clusters, reactants, products, complexes, and transition states were fully optimized with the Hartree−Fock method using a basis set of 6-31G** (denoted as HF/6-31G**). The optimized geometries were used to calculate the vibrational harmonic frequencies and zero-point energies. The minima are characterized with all real frequencies, whereas each transition state structure is characterized with one imaginary frequency. To verify that the transition state structure is the right saddle point connecting the corresponding reactants and products of interest, intrinsic reaction coordinate (IRC)[28] calculations were performed. To include electron correlation contributions, the MP2/6-31+G** single-point energy calculations (using the second-order Møller−Plesset perturbation theory with a larger basis set 6-31+G**) were performed with the optimized structures at the HF/6-31G** level of theory. Such an approach is designated by the standard notation MP2/6-31+G**//HF/6-31G**. Because Hartree−Fock theory is reasonably good in determining molecular structures,[29] the use of Hartree−Fock geometries and MP2 single-point energies could be expected to provide reliable total energies and activation energy barriers. In fact, the geometric structures of Si_2H_6 optimized using HF/6-31G** and MP2/6-31+G** are very close, with bond length deviation less than 0.5% and bond angle deviation within 0.2%; the total energy of Si_2H_6 at the MP2/6-31+G**//HF/6-31G** level is only 0.8 kcal/mol larger than that calculated at the higher level MP2/6-31+G**//MP2/6-31G**, and the energy barrier (44.6 kcal/mol) of the hydrogen abstraction reaction, $Si_2H_6 + H_2O \rightarrow Si_2H_5OH + H_2$, at the MP2/6-31+G**//HF/6-31G** level is only 0.6 kcal/mol higher than that (44.0 kcal/mol) at MP2/6-31+G**//MP2/6-31G**. The reactivity of the various reactions is judged by the evaluation of reaction energy barriers and reaction heats.

3. Results and Discussion

The hydrogen atoms on silicon cluster surfaces can be evaporated at high temperature. The stability of monohydride configurations can be simply determined by the Si−H bond energy as there is no direct interaction between neighboring hydrogen atoms. However, with dihydride or trihydride configurations evaporations of hydrogen molecules may be involved. On the other hand, the stability of hydrogenated silicon cluster surfaces may be determined by the reactions of the surface configurations with water molecules which could exist in the ambient environment of the silicon products. All these possibilities will be evaluated below.

3.1. Bond Energies of Silicon Hydrides. To evaluate the bond strength of the various hydride configurations on a silicon surface, we studied the Si−H bond energies of the SiH_x ($x = 1-3$) configurations, which are contained in the three models depicted in Figure 1a−c. Among the three models, the one shown in Figure 1a is saturated by mostly SiH_2 configurations (two SiH configurations are also present) on its surface, however, with different local environments. The model in Figure 1b contains SiH configurations at the dimerized Si(001) (2 × 1)-like configuration, whereas Figure 1c shows four SiH_3 configurations with different environments, along with some SiH and SiH_2. All the three structures and the ones in each of which one representative hydrogen atom was removed were fully optimized first at the HF/6-31G** level of theory, followed by single-point energy calculation at the MP2/6-31+G** level of theory. The bond energy is calculated as the difference between the total energy of the cluster, in which the specific hydrogen atom is removed plus the energy of a free hydrogen atom (spin polarization has been considered), and the total energy of the whole cluster. The bond energy so determined involves negligible basis set superposition error (BSSE),[30] as examined with a Si_2H_6 molecule for which the BSSE is less than 1% of the Si−H bond energy.

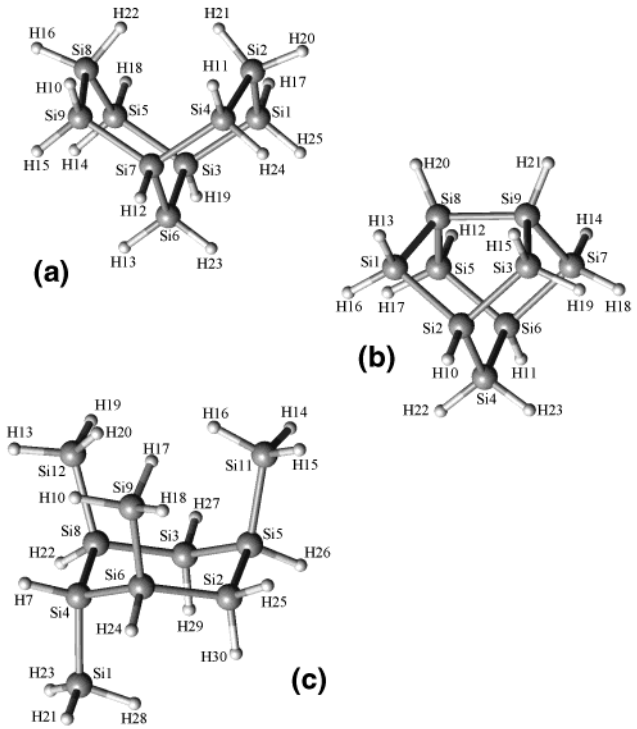

Figure 1. Three cluster models which contains silicon monohydride, silicon dihydride, and silicon trihydride configurations: (a) a model simulating a Si(001) (1 × 1)-like configuration; (b) a model simulating a Si(001) (2 × 1)-like configuration; (c) a model simulating a Si(111)-like configuration.

Table 1 shows the calculated bond energies of the various SiH_x ($x = 1-3$) configurations. Clearly, the bond energy shows a simple trend in that all the silicon monohydrides give the smallest bond energy ranging from 75.2 to ∼76.3 kcal/mol, whereas the silicon dihydride possesses bond energy around 77.9 to ∼78.9 kcal/mol and silicon trihydride is between 80.9 to ∼81.6 kcal/mol. The values obtained here are consistent with the experimental data of 82.6 kcal/mol for the Si−H bond energy[31] and the theoretical binding energies between 80.7 and 82.6 kcal/mol for hydrogen adsorbed on the silicon surface.[32] Therefore, the surface SiH_3 configuration is more stable with respect to thermal excitation. In Table 1 there is a correlation between the bond energies and the atomic net charges obtained by Mulliken population analysis. It is seen that a larger Si−H

TABLE 1: Si−H Bond Energies for H Atoms at Different Surface Locations of the Cluster Models Illustrated in Figure 1[a]

Si(001) (1 × 1)			Si(001) (2 × 1)			Si(111)		
H related	charge (au)	bond energy (kcal/mol)	H related	charge (au)	bond energy (kcal/mol)	H related	charge (au)	bond energy (kcal/mol)
H10(2)	−0.11	78.2	H11(1)	−0.09	76.3	H7(1)	−0.10	75.9
H12(1)	−0.10	75.2	H12(2)	−0.11	78.2	H13(3)	−0.12	80.9
H13(2)	−0.11	78.2	H17(2)	−0.11	78.9	H15(3)	−0.12	80.9
H15(2)	−0.12	78.4	H20(1)	−0.09	75.9	H16(3)	−0.13	81.4
H16(2)	−0.11	77.9	H22(2)	−0.11	78.2	H19(3)	−0.12	80.9
H22(2)	−0.12	78.6				H20(3)	−0.13	81.4
						H21(3)	−0.12	80.9
						H22(1)	−0.10	75.2
						H26(1)	−0.10	75.2
						H27(2)	−0.12	78.2
						H28(3)	−0.13	81.6
						H29(2)	−0.11	77.9

[a] The same labeling is used. The bond energy is the difference between the total energy of the cluster in which the specific hydrogen atom is removed plus the energy of a free hydrogen atom, and the total energy of the whole cluster. The total energies used were MP2/6-31+G** at the geometric structures fully optimized at the HF/6-31G** level of theory. Spin polarization has been considered in the calculation of the free hydrogen atom. The atomic charges were obtained according to Mulliken population analysis. The number in parentheses after the atom symbol of the related hydrogen is the "*x*" of the corresponding SiH_x configuration.

bond energy generally corresponds to a larger net charge at the hydrogen atom and thus an increased ionic interaction.

3.2. Energetics of H_2 Evaporation from the Surface of Silicon Hydrides. It was reported recently that hydrogen desorption of the trihydrides on Si nanowire surfaces occurred at ∼550 K and that of the dihydrides occurred at ∼650 K. At or above 750 K, all silicon hydride species began to desorb from the surfaces of the Si nanowire.[33] At around 850 K, Si nanowire surfaces were free of silicon hydride species. This result is in contradiction with the thermal stability results we described above. It was believed[33] that the poorer stability of silicon trihydride and dihydride are due to the formation of hydrogen molecules at high temperature. We therefore further studied such a chemical reaction of the dihydride configuration in Figure 1a and the trihydride configuration in Figure 1c (the trihydride at the Si1 site was replaced by a hydrogen atom). The results show that the chemical reactions leading to a H_2 evaporation require 81.9 and 86.9 kcal/mol for the dihydride and trihydride configurations, respectively, at the MP2/6-31+G*//HF/6-31G** level of theory. Clearly, the values are larger than any of the bond energies given above. To determine if a structural relaxation could lower the reaction energy barriers, we conducted calculations for the same evaporation reaction from the dihydride configuration but with a frozen geometry except for the two surface SiH_2 species (refer to Figure 1a). We found that the reaction energy barrier is slightly increased to a value of 82.3 kcal/mol, indicating that the evaporation energy of a H_2 molecule is indeed higher than that needed to break a Si−H bond. We will come back to this issue after presenting the results of water reaction with the various hydride configurations in order to provide a convincing explanation for the experimental observations reported in ref 33.

3.3. Energetics of Water Reaction with the Surface Silicon Hydrides. To study the reactions of the SiH, SiH_2, and SiH_3 configurations with water in the ambient environment, three cluster models, Si_9H_{15}−SiH, Si_8H_{14}−SiH_2, and Si_8H_{15}−SiH_3 are adopted, as shown in Figure 2a−c. They simulate, respectively, two hydrogenated unreconstructed Si(111)-like configurations containing monohydride and trihydride (Figure 2a,c) and a hydrogenated unreconstructed Si(001)-like configuration containing dihydride (Figure 2b). Moreover, a reconstructed Si(001) (2 × 1)-like configuration is also considered, because such a configuration is frequently observed in experiments. It is simulated using the cluster model, Si_9H_{14}, as shown in Figure 2d. With these models we have performed calculations at the MP2/6-31+G*//HF/6-31G** level of theory to study the reaction mechanisms of a water molecule with the various silicon hydrides (corresponding to hydrogen abstraction). The reaction routes are illustrated in Figure 2, and potential energy profiles are shown in Figure 3.

The reaction route of the hydrogen abstraction by water at the SiH configuration on the Si(111)-like configuration is shown in Figure 2a. It is seen that the reaction proceeds via Si_9H_{15}−SiH + H_2O → IC_a → TS_a → Si_9H_{15}−SiOH + H_2. For this hydrogen abstraction process, there appears at first a weak reactant-like complex, IC_a, 1.1 kcal/mol lower in energy than the reactants. The corresponding geometric parameters are listed in Table 2. At the IC_a the O−Si1 bond distance is as large as 4.083 Å, suggesting that the force for this weak complexation may be the dipole−dipole interaction. Then the system should pass through a transition state, TS_a, to go to the products. At the TS_a the O−Si bond distance between the attacking oxygen atom of H_2O and the attacked surface silicon atom (Si1) is 1.871 Å, longer by 12% than that in the product; the formed H−H bond is 1.124 Å, 53% longer than its value in the product. Thus, the Si−O bond would form at first, followed by the H−H bond formation. At the TS_a, one hydrogen atom (H5) on the silicon surface is drawn apart 1.886 Å from the surface silicon atom (Si1), 28% longer than its value in IC_a; meanwhile, another hydrogen atom (H4) leaves from the water with an O−H distance of 1.110 Å. For the two dissociated bonds, Si−H and O−H, the former would break first. Now, we can see clearly that water may attack the silicon surface via the Si−O bond formation and Si−H bond breaking, followed by the H−H bond formation. Although this is a complicated process, there exists only one transition state, indicating a one-step reaction for such a hydrogen abstraction. As shown in Figure 3a, the energy barrier of this reaction is 44.7 kcal/mol with respect to the reactants. The reaction is energetically favorable, because it is exothermic by about 13.7 kcal/mol.

For the Si(001) (1 × 1)-like configuration containing SiH_2, the hydrogen abstraction reaction has a similar mechanism as that for the above SiH configuration. The reaction pathway is Si_8H_{14}−SiH_2 + H_2O → IC_b → TS_b → Si_8H_{14}−SiHOH + H_2, as shown in Figure 2b. The reactant-like complex, IC_b, is 3.1 kcal/mol more stable than the reactants. As shown in Table 2, the O atom of water in the IC_b is 3.819 Å, far away from the attacked surface silicon atom (Si1). In the transition state, TS_b,

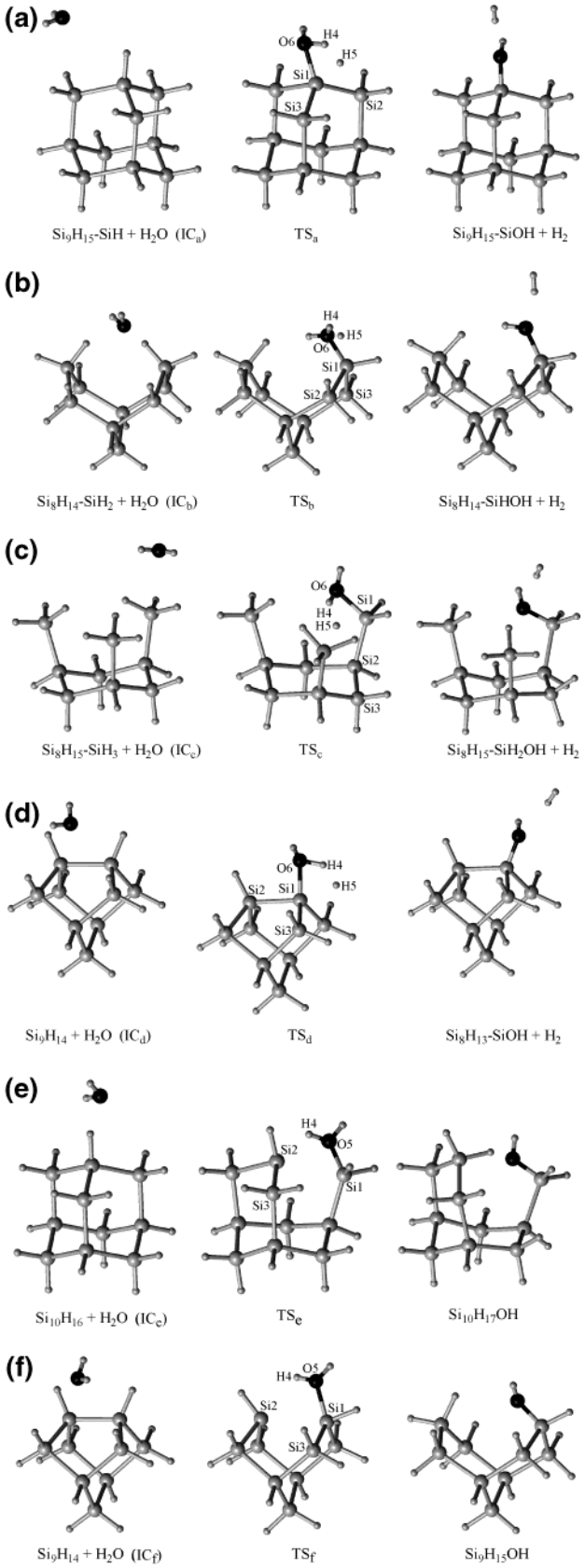

Figure 2. Schematic diagrams for water reactions with (a) a monohydride configuration, (b) a dihydride configuration, (c) a trihydride configuration, (d) a monohydride at a dimerized Si(001) (2 × 1) surface configuration, (e) a Si−Si bond on a Si(111)-like configuration, and (f) a Si−Si bond on a dimerized Si(001) (2 × 1)-like configuration.

the formed Si−O (1.849 Å) and H−H (1.132 Å) bonds are 11% and 54% longer than the ones in the product. And the Si−H

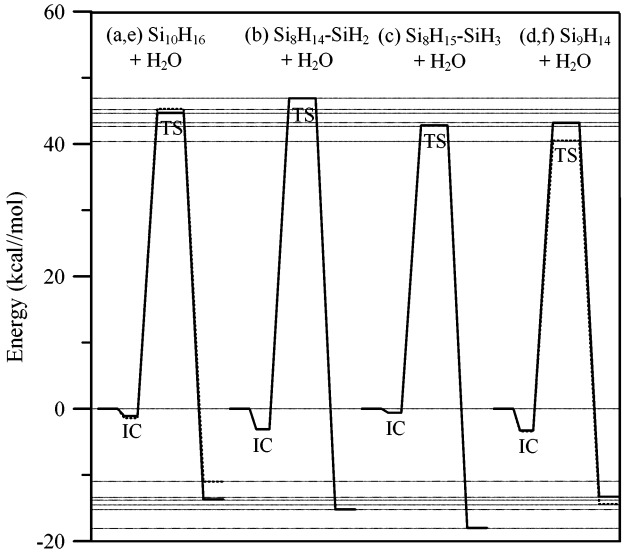

Figure 3. Energy profiles (kcal/mol) for water reaction with (a) a monohydride configuration, (b) a dihydride configuration, (c) a trihydride configuration, (d) a monohydride at a dimerized Si(001) (2 × 1)-like configuration, (e) a Si−Si bond on a Si(111)-like configuration (dashed line), and (f) a Si−Si bond on a dimerized Si(001) (2 × 1)-like configuration (dashed line).

(1.857 Å) and O−H (1.106 Å) bonds are drawn longer than their values in IC_b by 25% and 17%, respectively. It is shown that the transition state structure of TS_b is very similar to that of the TS_a of the previously discussed reaction. However, the Si−H in the present case is drawn longer whereas the H−H, Si−H, and O−H distances are closer to those in the reactants. Correspondingly, for the hydrogen abstraction on the surface SiH_2 configuration, the calculated energy barrier is 46.9 kcal/mol relative to the reactants, 2.2 kcal/mol larger than that for the SiH configuration (44.7 kcal/mol). On the basis of Hammond's principle, if a TS is more reactant-like, the reaction energy barrier would be lower; conversely, if the TS is more product-like, the barrier would be higher. Thus, we can deduce that the larger energy barrier for the SiH_2 configuration may be due to the shorter and thus more product-like Si−O bond in TS_b, which may be closely related to the more difficult deformation of the SiH_2 configuration (see Table 2).

A similar hydrogen abstraction reaction of the surface SiH_3 configuration with water is shown in Figure 2c. The reaction pathway is $Si_8H_{15}-SiH_3 + H_2O \rightarrow IC_c \rightarrow TS_c \rightarrow Si_8H_{15}-SiH_2-OH + H_2$. The reactant-like complex, IC_c, is only 0.6 kcal/mol more stable than the reactants. For this complex, the O−Si1 distance is 3.525 Å. In the transition state TS_c, the corresponding bonds, Si−O, H−H, Si−H, and O−H are 1.838 Å, 1.199 Å, 1.978 Å, and 1.073 Å, respectively, which are longer than their normal values by about 11%, 63%, 34%, and 14%, respectively, showing the trends of bond forming or breaking. TS_c has O−H and H−H bond distances considerably closer to those in the reactants along with the more product-like Si−H bonds than those in the transition state structures for water reaction at the Si−H and Si−H_2 configurations. The corresponding hydrogen abstraction on the SiH_3 surface has an energy barrier of 42.8 kcal/mol, lower than those for the SiH and SiH_2 configurations. Similarly, we can attribute this lower energy barrier to the smaller change of the H_2O structure in TS_c which relates to the easier deformation of Si−H bond on the SiH_3 surface.

Moreover, the reconstructed Si(001) (2 × 1)-like configuration was also considered. Similar to the above-discussed SiH, SiH_2, and SiH_3 configurations, this reaction occurs via Si_9H_{14}

TABLE 2: Geometrical Parameters for the Extrema on the Reaction Surfaces for the H_2 Abstractions Optimized at HF/6-31G** [a]

	IC_a	TS_a	IC_b	TS_b	IC_c	TS_c	IC_d	TS_d
Si1−O6	4.083	1.871	3.819	1.849	3.525	1.838	3.520	1.853
H4−H5	3.852	1.124	2.592	1.132	3.030	1.199	4.196	1.128
Si1−H5	1.478	1.886	1.480	1.857	1.477	1.978	1.479	1.881
O6−H4	0.943	1.110	0.943	1.106	0.943	1.073	0.944	1.112
O6Si1Si2	61.7	89.8	135.7	127.1	175.9	117.7	70.4	93.9
O6Si1Si2Si3	120.5	120.4	75.8	106.7	−27.7	−110.1	−94.8	−121.6
H4O6Si1	109.9	79.4	75.9	79.4	92.2	84.5	138.8	79.9
H4O6Si1Si2	57.7	−176.3	81.8	65.4	−44.0	72.7	48.4	−173.6
H5Si1Si2	110.4	156.5	108.3	86.9	109.7	82.9	113.6	160.8
H5Si1Si2Si3	120.5	119.5	122.3	165.5	−76.8	−51.8	−126.1	−129.5

[a] The corresponding structures are illustrated in Figure 2.

$+ H_2O \rightarrow IC_d \rightarrow TS_d \rightarrow Si_8H_{13}-SiOH + H_2$ (Figure 2d). A reactant-like complex, IC_d, also appears in the reaction surface, which is 3.3 kcal/mol more stable than the reactants. For the IC_d, the O atom of water is 3.520 Å away from the silicon atom (Si1) on the surface. In the transition state, TS_d, the formed Si−O (1.853 Å) and H−H (1.128 Å) bond distances are longer by 11% and 54%, respectively, than those in the products; the two dissociated bonds, Si−H (1.881 Å) and O−H (1.112 Å), are drawn longer by about 27% and 18%, respectively. These changes in bond lengths are similar to those for the SiH configuration. On this reconstructed surface, the energy barrier is calculated to be 43.2 kcal/mol with respect to the reactants, which is smaller than the related barriers at the SiH and SiH_2 configurations, indicating that the reconstructed silicon surface is more reactive than the corresponding unreconstructed structures.

According to the above studies, the hydrogen abstraction reaction of water with the surface hydrogen atom is generally similar for the SiH, SiH_2, and SiH_3 configurations on silicon surfaces as well as for the reconstructed silicon surface. The energy barriers for these reactions are very close and are much less than the bond energies for the corresponding silicon hydrides as listed in Table 1. Thus, it can be expected that these reactions are all likely to occur. Among the various reactions studied, the SiH_2 configuration on Si(001) surface is shown to be more unreactive and thus more stable than the SiH and SiH_3 configurations on Si(111) surfaces. On the contrary, the reconstructed surface configuration is more reactive than are the corresponding unreconstructed ones.

The above-described results well elucidate the experimental observation reported in ref 33 by correcting slightly the order of hydride stabilities to $SiH_3 < SiH < SiH_2$ (thus, the reverse order of hydride desorption). The correction would be considered reasonable if one reexamines Figure 4 in ref 33 where the three peaks from high to low wavenumbers correspond to the hydride configurations of SiH_3, SiH_2, and SiH, respectively, as confirmed by the ab initio calculations conducted in this work. It is noted that although the experiment in ref 33 was conducted in high vacuum, the coincidence between our theoretical results and the experimental observations indicates that water molecules were not efficiently pumped out. The absorption peaks relating to oxygen as seen in Figure 4 of ref 33 prove this elucidation.

3.4. Energetics of Water Reaction with the Surface Silicon Backbone. When water reacts with the silicon surfaces, the addition reaction, which results in a Si−Si bond breaking, may be another important reaction channel in addition to the hydrogen abstraction reaction. To study such a kind of reaction on a Si(111)-like configuration, we performed calculations for the reaction $Si_{10}H_{16} + H_2O \rightarrow Si_{10}H_{17}OH$, as illustrated in Figure 2e. It is shown that on the reaction route there exists one reactant-like complex (IC_e) and one transition state (TS_e). This reaction is also a one-step reaction. For the IC_e, the Si−O distance is as large as 4.054 Å, showing that this is a weak complex. In the TS_e, the formed Si−O bond is 1.886 Å, 14% longer than the Si−O bond in the product, whereas the formed Si−H bond is as large as 2.498 Å. On the other hand, the Si−Si bond being broken is 3.134 Å in TS_e, indicating that the Si−Si bond has been almost completely broken at the transition structure. Thus, the water addition reaction occurs with a Si−O bond being formed with a Si−Si bond being broken followed by a hydrogen migration from the O atom to the Si atom. The energy barrier of this reaction is calculated to be 45.3 kcal/mol with respect to the reactants as seen from Figure 3e, close to the corresponding hydrogen abstraction barrier (44.7 kcal/mol, see Figure 3a) for the SiH configuration. Therefore, the Si−Si bond can be easily broken by the addition of water onto the hydrogenated silicon surface. This kind of reaction channel can become competitive with the hydrogen abstraction reaction.

The addition reaction of water on the reconstructed Si(001) (2×1)-like configuration (Figure 2f), $Si_9H_{14} + H_2O \rightarrow Si_9H_{15}$-OH, was also studied. Similarly, the reaction route is $Si_9H_{14} + H_2O \rightarrow IC_f \rightarrow TS_f \rightarrow Si_9H_{15}OH$. The reactant-like complex (IC_f) is 3.4 kcal/mol more stable than the reactants. Correspondingly, the Si−O distance in the IC_f is 3.532 Å. In the transition state, TS_f, the formed Si−O bond length is 1.933 Å (larger than that of TS_e), and the formed Si−H bond is as large as 2.559 Å. Similar to the reaction as shown in Figure 2e, the Si1−Si2 bond (3.124 Å) has almost completely been broken at the TS_f. Because the TS_f is more reactant-like than the TS_e, the addition reaction on the reconstructed surface has a smaller energy barrier of 40.5 kcal/mol relative to that of the reactants. This energy barrier is actually the smallest one among all the considered reactions including the hydrogen abstractions.

3.5. Water Reactions on Different Hydrides of a Single Hydrogenated Silicon Cluster. In our recent work a size-dependent chemical reactivity of hydrogenated silicon clusters toward water has been explicitly demonstrated.[22] A unique trend of decreasing reactivity with decreasing cluster size has been deduced from reaction energetics, frontier orbital analysis, and chemical reaction rates for water reaction with both dihydride and trihydride silicon configurations. Accordingly, there is a risk when comparing the reactivity of hydrogenated silicon clusters illustrated in Figure 2, as the sizes of these clusters are not the same. Hopefully, the conclusions obtained with them are held as the sizes of these clusters are very similar. To have an unbiased conclusion, we conducted further calculations for water reactions on three different hydrides using the same hydrogenated silicon cluster. Figure 4 presents the reaction energy profiles and the transition state configurations of the corresponding reactions on the surfaces of a selected hydrogenated silicon cluster ($Si_{11}H_{18}$): (a) monohydride, (b) dihydride, and (c) trihydride.

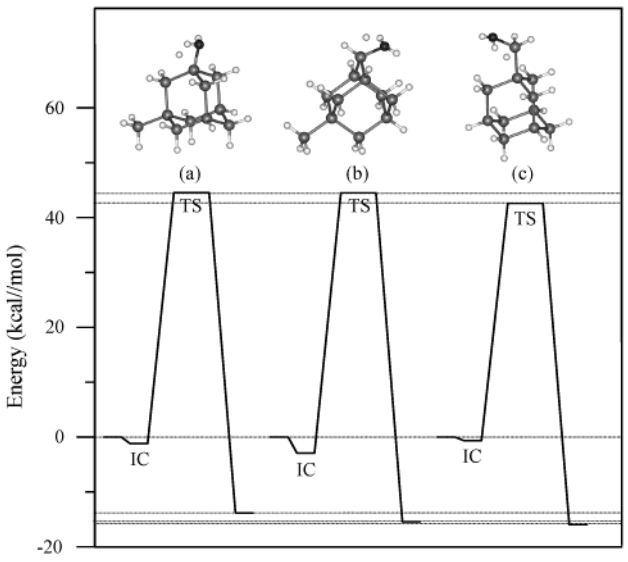

Figure 4. Energy profiles (kcal/mol) for water reaction with various silicon hydride configurations on the surface of a selected hydrogenated silicon cluster ($Si_{11}H_{18}$): (a) monohydride, (b) dihydride, and (c) trihydride. The structures of the corresponding transition states are shown above the energy profiles.

The reaction in Figure 4a involves a reactant-like complex, IC_a at first, which is 1.2 kcal/mol more stable than the reactants. The hydrogen abstraction on this SiH configuration has an energy barrier of 44.5 kcal/mol, very close to the value (44.7 kcal/mol in Figure 3a) obtained using $Si_{10}H_{16}$ (Figure 2a). The reaction is exothermic by about 13.8 kcal/mol (compared with the 13.7 kcal/mol obtained using $Si_{10}H_{16}$ in Figure 3a).

The reaction in Figure 4b on the SiH_2 configuration experiences at first a reactant-like complex, IC_b, of much larger stabilization energy of 2.9 kcal/mol. Afterward, the reaction undergoes a transition state with an energy barrier of 44.5 kcal/mol, the same as that for the SiH given in Figure 4a. The reaction is completed exothermically with a large energy of 15.4 kcal/mol released (compared with the 15.2 kcal/mol obtained using Si_9H_{16} in Figure 3b).

For the reaction at the SiH_3 configuration as illustrated in Figure 4c, the reactant-like complex, IC_c, is just 0.6 kcal/mol. The hydrogen abstraction on this trihydride configuration has a smaller energy barrier of 42.6 kcal/mol compared with the previous two larger values, indicating the ease of the water reaction on this trihydride configuration. The reaction is also exothermic with a large heat released (15.9 kcal/mol).

From this study it is concluded that the most inert reaction for the water molecule is still at the SiH_2 configuration as the energy barrier from the reactant-like complex to the transition state is the largest among the three cases, whereas the easiest reaction occurs at the SiH_3 configuration. These results are consistent with those illustrated in Figures 2 and 3.

3.6. General Discussion. According to the above results and discussion, it is found that for all the reactions considered here, the hydrogen abstraction and addition channels, the water addition reaction on the reconstructed configuration is the easiest, showing that the Si−Si backbone can easily be broken because of its considerably strained structure. Moreover, the reaction of water addition onto the hydrogenated Si(111)-like configuration which also leads to Si−Si bond breaking may possibly occur. It can be expected that the hydrogen abstraction reaction and the addition reaction of water on the unreconstructed silicon configurations would be two competitive reaction channels. Nevertheless, a dihydride configuration is shown to be the most stable one among the considered cases.

4. Conclusions

The wet oxidation in which the water molecule reacts with SiH_x ($x = 1-3$) configurations on silicon cluster surfaces is shown to be the main driving force for the degradation of hydrogenated silicon surfaces, which requires much less activation energy than that for hydrogen evaporation from the surface. The water reaction at SiH_2 is the most unfavorable one, whereas the easiest reaction may take place at the Si−Si dimer on a 2×1 reconstructed Si(001)-like configuration. On the hydrogenated unreconstructed silicon surface configurations, the hydrogen abstraction and the addition reaction of water may be two competitive reactions.

Acknowledgment. The work described in this article is supported by a Grant from the City University of Hong Kong (Project No. 7001340) and a Grant from the Research Grants Council of the Hong Kong Special Administrative Region, China (Project No. 9040633, e.g., City U 1011/01P).

References and Notes

(1) Chabal, Y. J. *Phys. Rev. B* **1984**, *29*, 3677.
(2) Chabal, Y. J.; Higashi, G. S.; Raghavachari, K.; Burrows, V. A. *J. Vac. Sci. Technol., A* **1989**, *7*, 2104.
(3) Sumitomo, K.; Kobayashi, T.; Shoji, F.; Oura, K.; Katayama, I. *Phys. Rev. Lett.* **1991**, *66*, 1193.
(4) Higashi, G. S.; Becker, R. S.; Chabal, Y. J.; Becker, A. J. *Appl. Phys. Lett.* **1991**, *58*, 1656.
(5) Higashi, G. S.; Chabal, Y. J.; Trucks, G. W.; Raghavachari, K. *Appl. Phys. Lett.* **1990**, *56*, 656.
(6) Hirashita, N.; Kinoshita, M.; Aikawa, I.; Ajioka, T. *Appl. Phys. Lett.* **1990**, *56*, 451.
(7) Higashi, G. S.; Chabal, Y. J.; Trucks, G. W.; Raghavachari, K. *Appl. Phys. Lett.* **1990**, *56*, 656.
(8) Ikeda, H.; Hotta, K.; Furuta, S.; Zaima, S.; Yasuda, Y. *Jpn. J. Appl. Phys.* **1996**, *35*, 1069.
(9) Canham, L. T. *Appl. Phys. Lett.* **1990**, *57*, 1046.
(10) Cullis, A. G.; Canham, L. T. *Nature (London)* **1991**, *353*, 335.
(11) Sham, T. K.; Jiang, D. T.; Couithard, I.; Lorimer, J. W.; Feng, X. H.; Tan, K. H.; Frigo, S. P.; Rosenberg, R. A.; Houghton, D. C.; Bryskiewicz, B. *Nature (London)* **1993**, *363*, 331.
(12) Buda, F.; Kohanoff, J.; Parrinello, M. *Phys. Rev. Lett.* **1992**, *69*, 1272.
(13) Tischler, M. A.; Collins, R. T.; Stathis, J. H.; Tsang, J. C. *Appl. Phys. Lett.* **1992**, *60*, 639.
(14) Morales, A. M.; Lieber, C. M. *Science* **1998**, *279*, 208.
(15) Zhang, R. Q.; Lifshitz, Y.; Lee, S. T. *Adv. Mater.* **2003**, *15*, *639* and references therein.
(16) Cooke, D. W.; Bennett, B. L.; Farnum, E. H.; Hults, W. L.; Sickafus, K. E.; Smith, J. F.; Smith, J. L.; Taylor, T. N.; Tiwari, P. *Appl. Phys. Lett.* **1996**, *68*, 1663.
(17) Yu, D. P.; Bai, Z. G.; Wang, J. J.; Zou, Y. H.; Qian, W.; Fu, J. S.; Zhang, H. Z.; Ding, Y.; Xiong, G. C.; You, L. P.; Xu, J.; Feng, S. Q. *Phys. Rev. B* **1999**, *59*, R2498.
(18) Daami, A.; Bremond, G.; Stalmans, L.; Poortmans, J. *J. Lumin.* **1998**, *80*, 169.
(19) Zhou, X. T.; Zhang, R. Q.; Peng, H. Y.; Shang, N. G.; Wang, N.; Bello, I.; Lee, C. S.; Lee, S. T. *Chem. Phys. Lett.* **2000**, *332*, 215.
(20) Becker, R. S.; Higashi, G. S.; Chabal, Y. J.; Becker, A. J. *Phys. Rev. Lett.* **1990**, *65*, 1917.
(21) Ma, D. D. D.; Lee, C. S.; Au, F. C. K.; Tong, S. Y.; Lee, S. T. *Science* **2003**, *299*, 1874.
(22) Zhang, R. Q.; Lu, W. C.; Lee, S. T. *Appl. Phys. Lett.* **2002**, *88*, 4223.
(23) Nachtigall, P.; Jordan, K. D.; Janda, K. C. *J. Chem. Phys.* **1991**, *95*, 8652.
(24) Weldon, M. K.; Queeney, K. T.; Gurevich, A. B.; Stefanov, B. B.; Chabal, Y. J.; Raghavachari, K. *J. Chem. Phys.* **2000**, *113*, 2440.
(25) Teraishi, K.; Takaba, H.; Yamada, A.; Endou, A.; Gunji, I.; Chatterjee, A.; Kubo, M.; Miyamoto, A.; Nakamura, K.; Kitajima, M. *J. Chem. Phys.* **1998**, *109*, 1495.

(26) Ranke, W.; Xing, Y. R. *Surf. Sci.* **1997**, *381*, 1.
(27) Frisch, M. J.; Trucks, G. W.; Schlegel, H. B.; Scuseria, G. E.; Robb, M. A.; Cheeseman, J. R.; Zakrzewski, V. G.; Montgomery, J. A., Jr.; Stratmann, R. E.; Burant, J. C.; Dapprich, S.; Millam, J. M.; Daniels, A. D.; Kudin, K. N.; Strain, M. C.; Farkas, O.; Tomasi, J.; Barone, V.; Cossi, M.; Cammi, R.; Mennucci, B.; Pomelli, C.; Adamo, C.; Clifford, S.; Ochterski, J.; Petersson, G. A.; Ayala, P. Y.; Cui, Q.; Morokuma, K.; Malick, D. K.; Rabuck, A. D.; Raghavachari, K.; Foresman, J. B.; Cioslowski, J.; Ortiz, J. V.; Stefanov, B. B.; Liu, G.; Liashenko, A.; Piskorz, P.; Komaromi, I.; Gomperts, R.; Martin, R. L.; Fox, D. J.; Keith, T.; Al-Laham, M. A.; Peng, C. Y.; Nanayakkara, A.; Gonzalez, C.; Challacombe, M.; Gill, P. M. W.; Johnson, B. G.; Chen, W.; Wong, M. W.; Andres, J. L.; Head-Gordon, M.; Replogle, E. S.; Pople, J. A. *Gaussian 98*, revision A.7; Gaussian, Inc.: Pittsburgh, PA, 1998.
(28) Gonzalez, C.; Schlegel, H. B. *J. Phys. Chem.* **1990**, *94*, 5523.
(29) Levy, M.; Perdew, J. P. *J. Chem. Phys.* **1986**, *84*, 4519.
(30) Hobza, P.; Zahradnik, R. *Chem. Rev.* **1988**, *88*, 871.
(31) Koehler, B. G.; Mak, C. H.; Arthur, D. A.; Coon, P. A.; George, S. M. *J. Chem. Phys.* **1988**, *89*, 1709.
(32) Jing, Z.; Whitten, J. L. *J. Chem. Phys.* **1992**, *46*, 9544.
(33) Sun, X. H.; Wang, S. D.; Wong, N. B.; Ma, D. D. D.; Lee, S. T. *Inorg. Chem.* **2003**, *42*, 2398.